

## A Colorimetric and Fluorescent Dual-Signal Sensor for Detecting Lipase Activity Based on Inner Filter Effect

Ting Du,<sup>a</sup> Fu Zhang,<sup>a</sup> Ling Jiang<sup>b</sup> and Danbi Tian<sup>\*a</sup>

<sup>a</sup>School of Chemistry and Molecular Engineering, Nanjing Tech University, Nanjing 211880, China

<sup>b</sup>College of Food Science and Light Industry, Nanjing Tech University, Nanjing 211880, China

We developed a colorimetric and fluorescence dual-signal sensor for detecting lipase activity based on methyl thioglycolate (MT) functionalized gold nanoparticles (MT-AuNPs) and CdS quantum dots (CdS QDs). It is the first time that was developed a dual-signal sensing strategy for lipase activity based on the inner-filter effect (IFE) between MT-AuNPs and CdS QDs. This probe system (MT-AuNPs + CdS QDs) is sensitive and has selective response to the concentration of the lipase, and MT-AuNPs and CdS QDs played as transducer and fluorescer, respectively. The addition of lipase triggered the accumulation and change of color in CdS QDs and MT-AuNPs solution, it also makes the fluorescence intensity of CdS QDs significantly recover. The limit of detection (LOD) was as low as 0.039  $\mu\text{g mL}^{-1}$  for colorimetric detection as well as 0.012  $\mu\text{g mL}^{-1}$  for the fluorescence method. This method has been successfully used in the detection of commercial lipases. We believe it would open up a new path for the sensitive and high throughput lipase assay using nanobiosensor.

**Keywords:** lipase, dual-signal, biosensor, inner filter effect

### Introduction

The lipases (EC 3.1.1.3), triacylglycerol hydrolases, occupy the major share of the biotechnologically relevant enzyme.<sup>1</sup> They can catalyze the carboxylic ester hydrolyzation, esterification, interesterification and transesterification reaction in nonaqueous environment.<sup>2-4</sup> This multi-function confers lipases a huge potential applications in the food, detergent, and pharmaceutical industries.<sup>5-8</sup> In clinical diagnosis, lipase activity is closely in connection with multifarious pancreatic diseases, and the detecting lipase in human serum can be specific and sensitive for acute pancreatitis.<sup>9</sup> In discovering and developing their novel applications, lipase activity is an important parameter not only in screening the best performant lipase in industry but in developing novel pharmaceutical and medical diagnostic methods.

As we know, it is still an underdeveloped field for difficult strategy design due to its water-insoluble substrates as well as the water-oil reaction interface. Shi *et al.*<sup>10,11</sup> assembled a fluorescent probe to detect lipase activity based on aggregation-induced emission effect (AIE). These probes

have the superiorities of high sensitive and low detection of lipase activity, but these strategies could only detect lipase in the water/organic phase. The process of detection was complicated, which could not overcome the problem of lipase oil-water interface catalysis. Qiao *et al.*<sup>12</sup> designed and assembled an *in vivo* self-assembled fluorescent probe for lipase activity detection. Although this method broke the binding of lipase catalysis at the oil-water interface, it still required the use of organic solvents that are mutually soluble with water.

Quantum dots (QDs) attracted special attention because of their unique optical properties, such as high fluorescence quantum yield (QY),<sup>13</sup> efficient broadband absorption with a narrowband fluorescence spectrum.<sup>14,15</sup> Its excellent advantages make it diffusely applied to cell labeling, biosensing, intracellular imaging and medical diagnosis.<sup>16-18</sup> The inner-filter effect (IFE) or fluorescence resonance energy transfer effect (FRET) exists between dispersed gold nanoparticles (AuNPs) and QDs, which can quench the fluorescence of QDs. Incorporating these principles, a new platform for enzyme assay was developed.<sup>19-21</sup>

IFE is regarded as a competent way for improving the conversion efficiency of the absorption signals into fluorescence signals.<sup>22</sup> The FRET-based approaches are highly dependent on the distance between fluorophores and absorbers, while the IFE-based systems do not need any

\*e-mail: danbi@njtech.edu.cn

Editor handled this article: Fernando C. Giacomelli (Associate)

covalent linkage between absorber and fluorophore.<sup>23,24</sup> In the field of QDs-based IFE enzyme assays, the complex modifying process on the surfaces of particles could be avoided and a more pronounced fluorescence signal can offer high sensitivity.<sup>25</sup>

In recent years, the effort of our group was devoted to the research of measuring lipase activity.<sup>26-28</sup> Zhang *et al.*<sup>29</sup> have developed a fluorescent probe for lipase detection based on enzyme-controlled CdS QDs growth *in situ*. It was verified that the methyl thioglycolate (MT) could be employed as a substrate of lipase and the carboxyl ester bond in MT could be hydrolytic cleaved to form mercaptoacetate catalyzed by lipase. Xue *et al.*<sup>30</sup> have reported that hydrogen bonds formed between thioglycolic acid attached CdTe QDs and citrate-covered AuNPs at pH 5-7. Moreover, Bahram and co-workers<sup>31</sup> have established a probe system for sensitive assay of arginine on the basis of the IFE effect between AuNPs and CdS QDs. Inspired by the literature and our previous work,<sup>29</sup> we designed a colorimetric and fluorescent dual-signal sensing method for detection of lipase activity. It does not need expensive recognizing elements and complicated modifying methods on the surface of AuNPs and QDs. The dual-signal sensing method is able to read out lipase activity visually and fluorescently and thus offer increased accuracy and diversity. The high sensitivity towards lipase was carried out with limit of detection (LOD)  $0.039 \mu\text{g mL}^{-1}$  for colorimetric detection as well as  $0.012 \mu\text{g mL}^{-1}$  for fluorescence method. This method has been successfully used in the detection of commercial purchased lipase samples. It opened a new way for facile and high throughput lipase activity detection, which is special benefit in industrial lipases optimization.

## Experimental

### Materials

All chemicals and reagents were directly available on the market and of analytically pure grade without further purification. Cadmium nitrate ( $\text{Cd}(\text{NO}_3)_2 \cdot 4\text{H}_2\text{O}$ ) and sodium sulfide ( $\text{Na}_2\text{S} \cdot 9\text{H}_2\text{O}$ ) were purchased from Shanghai Lingfeng Chemical Reagent (Shanghai, China), and methyl thioglycolate (MT) from Sinopharm Holding Co. LTD (Shanghai, China). L-Cysteine (L-cys), concentrated hydrochloric (HCl), concentrated nitric acid ( $\text{HNO}_3$ ), trihydroxy-methyl-amino-methane (Tris), disodium hydrogen phosphate ( $\text{Na}_2\text{HPO}_4$ ), potassium dihydrogen phosphate ( $\text{NaH}_2\text{PO}_4$ ), sodium chloride (NaCl), potassium chloride (KCl), acetone ( $\text{C}_3\text{H}_6\text{O}$ ), sodium citrate ( $\text{Na}_3\text{C}_6\text{H}_5\text{O}_7 \cdot 2\text{H}_2\text{O}$ ), chloroauric acid tetrahydrate ( $\text{HAuCl}_4 \cdot 3\text{H}_2\text{O}$ ) were all purchased from Aladin Chemistry

(Shanghai, China). Lipase from porcine pancreatic (PPL), *Candida rugosa* (CRL), *Ferrodobacterium nodosum* (FNL) and pseudomonas (PSL), and Novozymes-435 lipase (Novozymes435) were all purchased from Sigma-Aldrich (Shanghai, China). Phosphate buffer solution (PBS) was purchased from Shanghai Yuanye Biotechnology (Shanghai, China). All solutions were prepared with ultrapure water, which has resistivity of  $18.2 \text{ M}\Omega \text{ cm}$  during experiment.

### Apparatus

The ultraviolet-visible (UV-Vis) absorption spectra were measured with a LAMBDA950 UV-Vis NIR spectrophotometer (PerkinElmer, Shanghai, China). The fluorescence spectra were recorded by SpectraMax M3 multifunctional micrometer (Molecular Devices, Silicon Valley, USA). Both the excitation and emission slit widths were fixed at 5 nm and the excitation wavelength was 360 nm. The morphologies of samples were characterized by transmission electron microscope with an acceleration voltage of 100 kV (JEOL, Tokyo, Japan). We used a 90Plus PLAS for measuring zeta potential values (Brookhaven, New York, USA) and Milli-Q system (Millipore, Darmstadt, Germany) to obtain ultrapure water.

### Synthesis of CdS QDs

The synthesis of CdS QDs was performed on the basis of the literature with some modifications.<sup>32</sup>  $\text{N}_2$  was injected into 50 mL Tris-HCl (0.1 M, pH 8.5) for 60 min, and then 6 mL L-Cys (3 mM) and 3 mL  $\text{Cd}(\text{NO}_3)_2 \cdot 4\text{H}_2\text{O}$  (2.25 mM) were added, after stirring the mixed solution for 5 min, 6 mL  $\text{NaS} \cdot 9\text{H}_2\text{O}$  (1.5 mM), and ultra-pure water were added to make the total volume of the mixed solution 100 mL. The solution was stirred at room temperature for 24 h under  $\text{N}_2$  atmosphere, to obtain L-Cys-coated CdS QDs. The CdS QDs were ultrasonically treated, cleaned with  $\text{C}_3\text{H}_6\text{O}$ , and stored in a Tris-HCl (0.1 M, pH 7.4) buffer solution. The CdS QDs obtained by this method can be stored at  $4^\circ\text{C}$  for a long time, and the concentration of CdS QDs is about  $30 \mu\text{M}$  according to the theoretical calculation of Peng and co-workers.<sup>33</sup>

### Synthesis of MT-AuNPs

The synthesis of gold nanoparticles (AuNPs) was based on the reaction of  $\text{HAuCl}_4 \cdot 3\text{H}_2\text{O}$  with sodium citrate as previously reported.<sup>34</sup> The average particle size of AuNPs obtained was about 13 nm. According to Haiss *et al.*,<sup>35</sup> the concentration of AuNPs were about  $3.96 \text{ nM}$ . 10 mL of the prepared AuNPs solution, and

1 mL methyl thioglycolate (MT,  $4 \times 10^{-6}$  mol L<sup>-1</sup>) were mixed to stir and react continuously for 24 h in dark. The excess of MT was removed by repeated centrifugation (12,000 rpm, 10 min) and the prepared precipitate was MT-AuNPs, which were dissolved in 10 mL ultra-pure water and refrigerated at 4 °C.

### Detection of lipase activity

A series of lipase solutions with different concentration (0-45  $\mu\text{g mL}^{-1}$ ) were prepared with PBS buffer (2 mM, pH 6.0). Lipase solutions were mixed with CdS QDs (3  $\mu\text{M}$ ), MT-AuNPs (1.61 nM) and PBS buffer (2 mM, pH 6.0), and the ultimate volume was 1000  $\mu\text{L}$ . The resulting solution was taken in a constant temperature water bath at 45 °C with oscillating incubation. After 14 min, the absorption spectra and fluorescence spectra of the mixed solution were determined.

### Lipase assay in commercial purchased samples

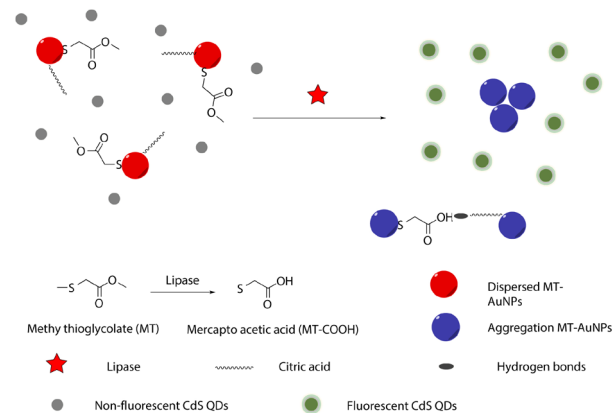
Five commercially purchased lipase samples (Novozymes 435, PPL, CRL, FNL, PSL) were used to verify the practicality and accuracy of this dual-signal strategy. Lipase samples were dispersed with PBS buffer (20  $\mu\text{g mL}^{-1}$ ). Adding lipase samples, CdS QDs (3  $\mu\text{M}$ ), MT-AuNPs (1.61 nM) and PBS buffer (2 mM, pH 6.0) into Eppendorf tube, and the ultimate volume was 1000  $\mu\text{L}$ . The resulting solution was in a constant temperature water bath at 45 °C for 14 min with oscillating incubation. Then, it was performed absorbance and fluorescence detection on the mixed solution. The results detected by this dual-signal strategy was compared with the detection of pH-stat potentiometric titration (equations S1 and S2, Supplementary Information (SI) section).

## Results and Discussion

### Mechanism of the dual-signal assay for lipase activity

The principles of the colorimetric and fluorescent assay for lipase activity were illustrated in Scheme 1. We used CdS QDs as the fluorescer and the MT-AuNPs as the absorbers. Because the absorption spectrum of dispersive MT-AuNPs adequately overlapped the fluorescent excitation spectrum of the CdS QDs, the fluorescence of CdS QDs was quenched by the dispersive MT-AuNPs in the solution due to IFE.<sup>35</sup>

The design of this sensor strategy for lipase activity detection is based in the principle that the lipase could catalyze the hydrolysis of the carboxylic ester bond in



**Scheme 1.** Schematic illustration of the mechanism of sensing the activity of lipase based on IFE.

MT on the surface of MT-AuNPs, producing hydrolytic residual mercaptoacetate.<sup>29</sup> Because the carboxyl group in mercaptoacetate and citrate group on the surface of the AuNPs, which is synthesized by chloroauric acid and citrate salt, can be partly protonated in weakly acidic solution, the hydrogen bonds, which could triggered the aggregation of the MT-AuNPs, can be formed between them, so the solution color change.<sup>30</sup> Furthermore, the aggregation of the MT-AuNPs can trigger the fluorescence of CdS QDs exponentially recovered. Upon adding lipase, both fluorescence emission intensity of the CdS QDs and the colorimetric absorbance of MT-AuNPs significantly changed along with the color of mixed solution from red to purple. The lipase activity could be detected by using both colorimetric and fluorescent dual-signal sensor in the range of 0-45  $\mu\text{g mL}^{-1}$ .

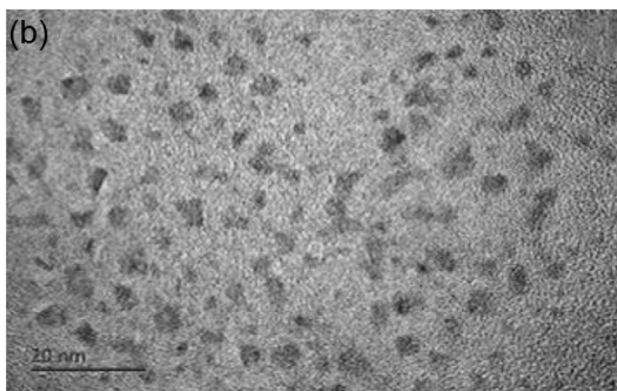
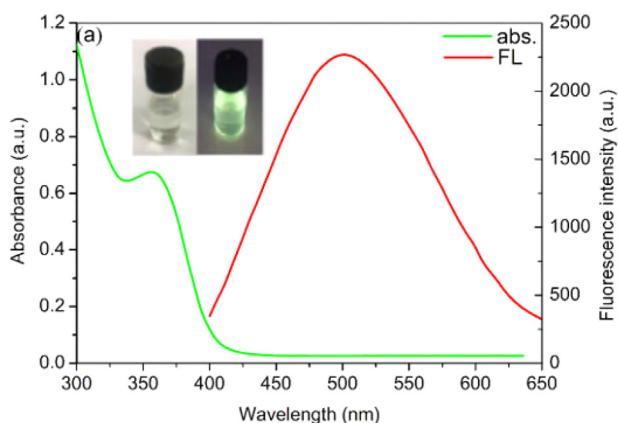
### Characterization of CdS QDs and MT-AuNPs

Figure 1a showed the UV-Vis absorption and fluorescence emission of the CdS QDs. There is an absorbance peak at 360 nm and a fluorescence peak at 505 nm, respectively. The well-shaped peak indicates a homogeneous distribution of CdS QDs with diameter of 2.3 nm. The diameter is consistent with transmission electron microscopy (TEM, Figure 1b).

The absorbance of MT-AuNPs and fluorescence of CdS QDs stored darkly at 4 °C for 20 days were measured to confirm the stability of them. The properties of MT-AuNPs and CdS QDs were retained over 80% (Figure S1, SI section).

### Fluorescence quenching effect of MT-AuNPs on CdS QDs

Figure 2 showed that the absorption spectrum of MT-AuNPs and the fluorescence emission spectrum of CdS QDs overlap commendably, implying that IFE



**Figure 1.** (a) The absorbance and fluorescence emission spectrum of CdS QDs (inset: the photographs of CdS QDs solution under daylight and UV light) and (b) TEM image of CdS QDs.

might occur.<sup>36-39</sup> Along with increasing concentration of MT-AuNPs, the emission intensity of CdS QDs decreased gradually. When the concentration of MT-AuNPs was up to  $1.84 \times 10^{-9}$  M, the fluorescence emission from CdS QDs was quenched more than 65% (Figure 3), suggesting that the MT-AuNPs might effectively quench fluorescence of the CdS QDs in a concentration depending way.

The zeta potential ( $\xi$ ) of MT-AuNPs and CdS QDs were measured (Figure S2, SI section) and the  $\xi$  value of MT-AuNPs and CdS QDs were  $-18.75$  and  $-12.97$  V, respectively, at pH 7.4. Since both of the particles were negative charged, it could be deduced that there was a strong electrostatic repulsion effect between them. When the distance between receptor-donor is 1-10 nm,<sup>40</sup> the fluorescence quenching caused by FRET is possible, and the electrostatic repulsive between MT-AuNPs and CdS QDs cannot well guarantee this condition.

The fluorescence lifetime of CdS QDs with and without MT-AuNPs was investigated. From Figure S3 (SI section), it is evident that the average lifetime of the CdS QDs is not affected by MT-AuNPs, suggesting that the complex compound could not be formed. This phenomenon confirmed that the fluorescence decrease was made by IFE between the CdS QDs and MT-AuNPs, rather than FRET.<sup>41,42</sup>

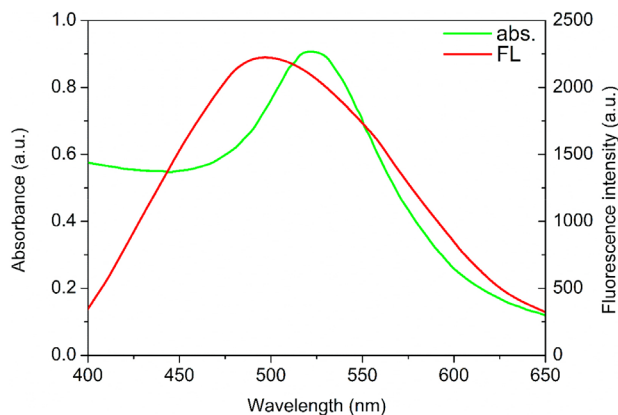


**Figure 2.** The absorption spectrum of MT-AuNPs and fluorescence emission spectrum of CdS QDs.

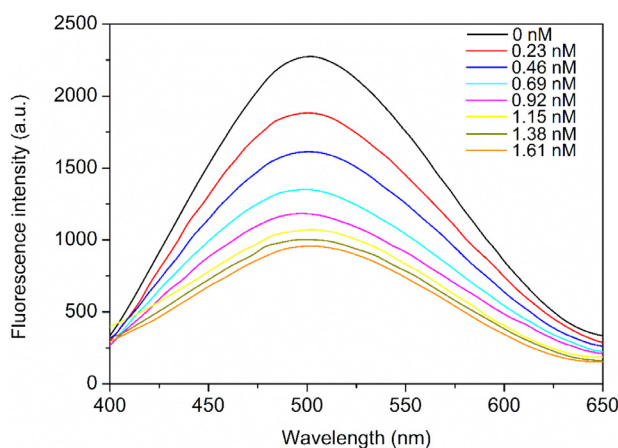


**Figure 3.** The fluorescence emission spectra of CdS QDs in presence of various MT-AuNPs concentrations (MT-AuNPs, 0-1.61 nM; CdS QDs, 3  $\mu$ M).

#### IFE-based QDs emission response to lipase activity

It is reasonably expected that the IFE process can be modulated through congregating the AuNPs. To illustrate this principle for lipase activity detection, the absorbance and fluorescence spectra of MT-AuNPs and CdS QDs were investigated in detail with and without lipase. Figure 4 shows that the absorption peak of CdS QDs at 360 nm remained unchanged with the addition of lipase, demonstrating that the absorption of CdS QDs is independent on the lipase (curves a, b). The curves c and e demonstrated that there was not any interaction between CdS QDs and MT-AuNPs. Upon the addition of lipase, the absorption peak of MT-AuNPs at 520 nm decreased as a new visible absorption peak centered at 650 nm increased (curve f), indicating that the aggregation of MT-AuNPs was resulted from lipase. The same experiment was carried on in MT-AuNPs + CdS QDs solution, the results kept unchanged (curve d). From these experiments we can see that in colorimetric detection the aggregation of MT-AuNPs was induced only by lipase and the presence of CdS QDs

did not affect the modulating effects. It is also confirmed by images of TEM (Figure 5).

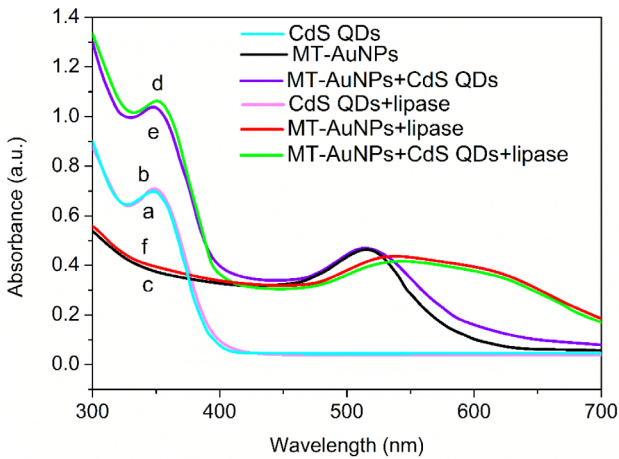


**Figure 4.** The effects of lipase on absorption of CdS QDs, MT-AuNPs and MT-AuNPs + CdS QDs (MT-AuNPs, 1.61 nM; CdS QDs, 3  $\mu$ M).

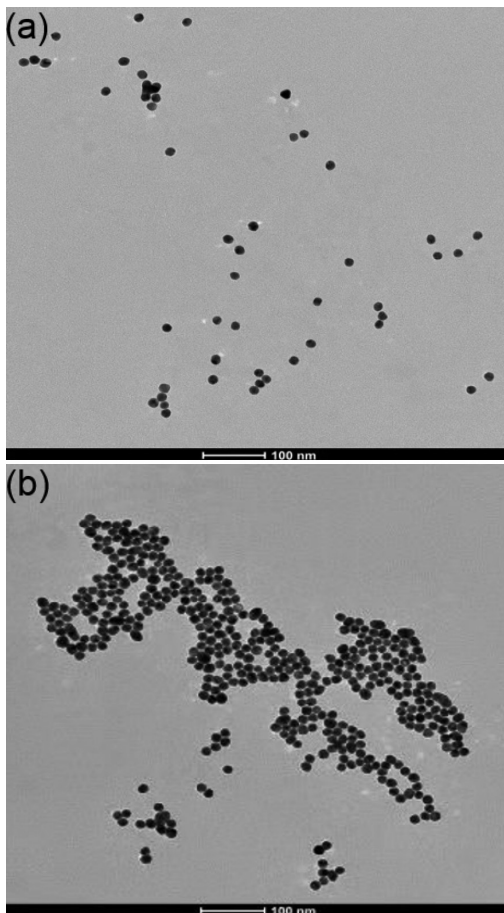


**Figure 5.** (a) TEM images of MT-AuNPs without lipase and (b) with lipase.

To make sure the expected detecting performance, the fluorescence response of the IFE-based assay for lipase was investigated. Figure 6 showed that the maximum

fluorescence emission peak of CdS QDs was 505 nm, no changes were observed in the presence and absence of the lipase, showing that the fluorescence of CdS QDs is independent on the lipase. When CdS QDs and MT-AuNPs were mixed, the fluorescence emission was obviously quenched. In the presence of the lipase, the fluorescence of the mixture solution was resumed significantly, confirming that the fluorescence recovery might entirely derive from the interaction between lipase and MT-AuNPs, which controlled the IFE and further affected the fluorescence of CdS QDs.

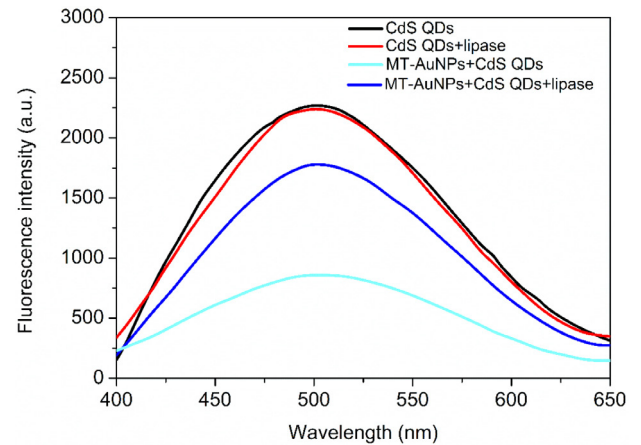


**Figure 6.** The effects of lipase on fluorescence emission of CdS QD and CdS QDs + MT-AuNPs (MT-AuNPs, 1.61 nM; CdS QDs, 3  $\mu$ M).

#### Optimization of experimental conditions

The ratio value ( $A_{650}/A_{520}$ ) of the absorbance is used to quantify the AuNPs aggregation process.<sup>43,44</sup> Since the concentration of MT may affect AuNPs aggregating performance, the effect of MT concentration was studied. As shown in Figure 7, the  $A_{650}/A_{520}$  almost unchanged with the increasing MT concentration in the range of 1–4  $\mu$ M and started to increase above 4  $\mu$ M. The higher MT concentration

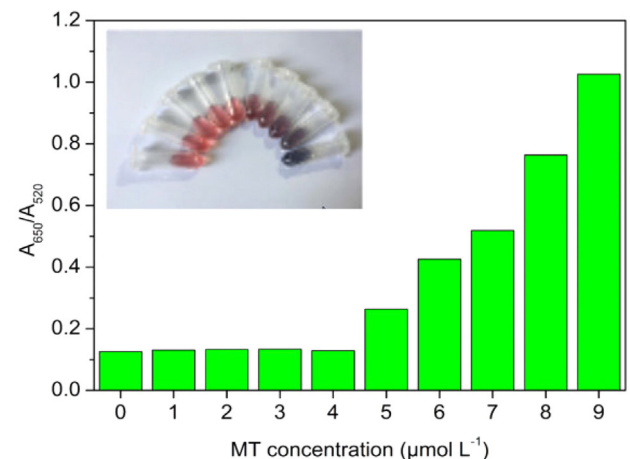


**Figure 7.** The value of  $A_{650}/A_{520}$  of MT-AuNPs in the presence of different concentrations of MT (inset: the photographs of MT-AuNPs visual color).

could induce the aggregation of the MT-AuNPs, while it could result in the decrease the IFE effect between CdS QDs and MT-AuNPs consequently. Thus, 4  $\mu\text{M}$  MT was chosen as the optimum MT concentration. This concentration of MT can guarantee that the MT-AuNPs are still in disperse state and IFE could occur sensitively.

pH is an important factor in this work. It not only affects the lipase activity significantly but affects the formation of hydrogen bonds between MT-AuNPs and CdS QDs. The optimum pH for the experiment was investigated. According to our previous research,<sup>29</sup> the optimum pH for lipase is about 8.0, but it does not benefit the formation of hydrogen bond. We need to consider these two effects as a whole in order to achieve a good result. According to the results in Figure S4 (SI section), the optimum pH was 6.0 both in  $A_{650}/A_{520}$  and fluorescence detections.

The influence of the ionic strength, the reaction temperature and reaction time were also investigated (Figures S5, S6, S7, SI section), the results showed that the type of the buffer was PBS with concentration 0.02 mol L<sup>-1</sup>, the optimum reaction temperature was 45 °C and the incubation time was 14 min.

#### Sensitivity of the assay

Under the optimum experimental conditions, the sensitivity of the lipase was investigated by UV-Vis spectrophotometry. In Figure 8a, when lipase concentration increased (0-45  $\mu\text{g mL}^{-1}$ ), the absorbance of MT-AuNPs gradually decreased at 520 nm and increased at 650 nm. Meanwhile,  $A_{650}/A_{520}$  ratio as a function of the concentration of lipase, was plotted in Figure 8b, with correlation coefficient ( $R^2$ ) of 0.9988. In this process, the detections were repeated three times. The LOD of the lipase reached 0.039  $\mu\text{g mL}^{-1}$ , which was calculated by the relevant formula ( $\text{LOD} = 3s/\text{slope}$ ). In the formula, the  $s$  value was  $3.52 \times 10^{-4}$ , it represents the standard deviation of the signal measured by the three distinct blank samples.

Moreover, basing on the IFE between MT-AuNPs and CdS QDs, a fluorescence method for lipase assay was carried on as well. As can be seen from Figure 9a, fluorescence of CdS QDs gradually increased with the lipase concentration increasing, corresponding to the increasing absorbance of MT-AuNPs at 520 nm. In Figure 9b, the fluorescence intensities of CdS QDs were dependent on concentration, the higher concentrations of lipase the more fluorescence recovery could be made. The calibration curves of the relative fluorescence intensity ( $F-F_0$ ) against lipase concentrations (0.1-45  $\mu\text{g mL}^{-1}$ ) were obtained. The LOD ( $3\sigma/s$ ) for lipase was found to be 0.012  $\mu\text{g mL}^{-1}$  ( $n = 3$ ), which was much lower than the assay reported previously.

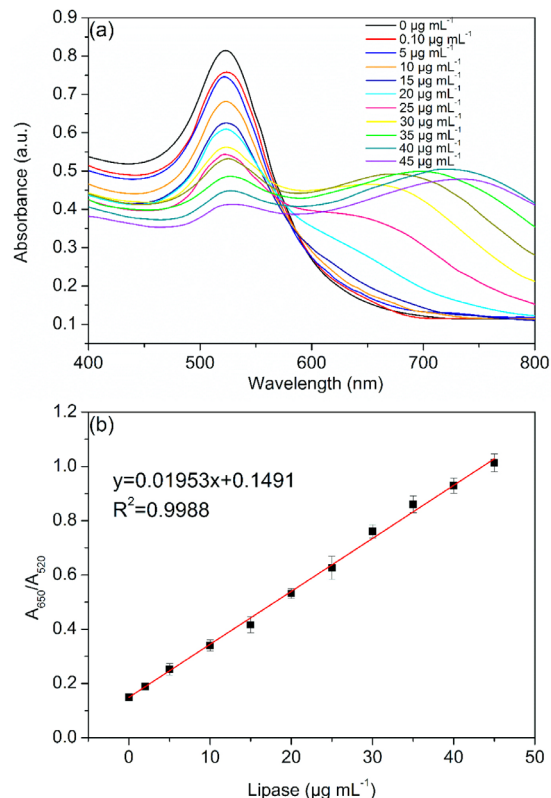


**Figure 8.** (a) The absorption spectrum of MT-AuNPs in the presence of different lipase concentration (0-45  $\mu\text{g mL}^{-1}$ ); (b) the relationship between the  $A_{650}/A_{520}$  and lipase concentrations.

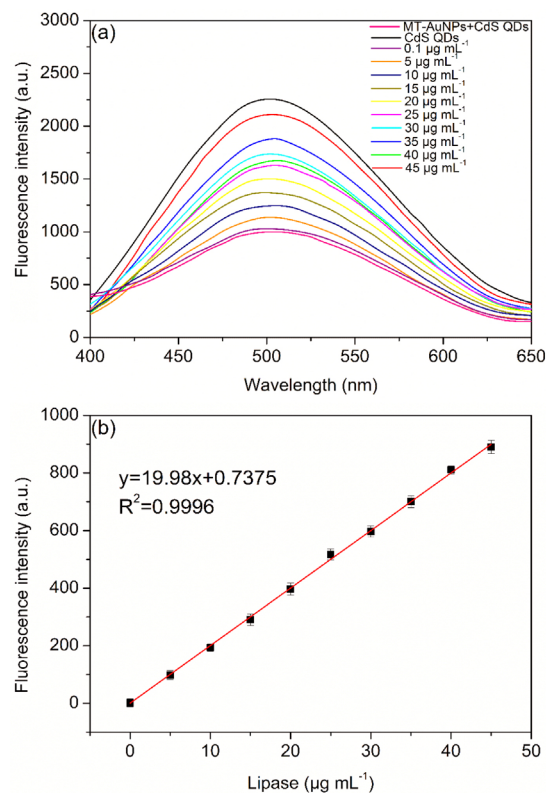


**Figure 9.** (a) The fluorescence emission spectra of MT-AuNPs + CdS QDs in the presence of increasing concentrations of lipase (0-45  $\mu\text{g mL}^{-1}$ ); (b) the relationship between the  $F-F_0$  and lipase concentrations.

## Practical application

This dual-signal lipase detection strategy was applied to the detection of five commercial lipases (Novozymes435, PPL, CRL, FNL and PSL). We added identical concentration of lipase ( $20 \mu\text{g mL}^{-1}$ ) to the mix solution of MT-AuNPs and CdS QDs, and incubated in shock for 14 min. Then, the  $A_{650}/A_{520}$  of MT-AuNPs and fluorescence of CdS QDs were measured, and the results were shown in Figure 10. We conclude that the lipase activity decreases sequentially (Novozymes435 > PPL > CRL > FNL > PSL). In the meantime, pH-stat potentiometric titration method was used to survey these five commercial lipase (Table 1). The sequence of lipase samples detected by the dual-signal assay was consistent with that of the conventional titration method. It demonstrates that the assay designed by us can replace the traditional methods for a high throughput detection of lipase activity.

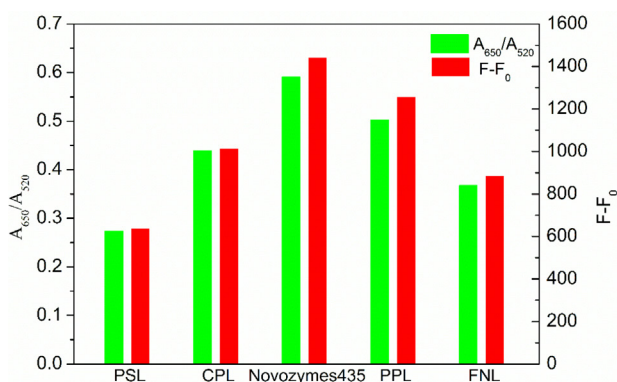


**Figure 10.** The  $A_{650}/A_{520}$  and  $F-F_0$  intensity of MT-AuNPs + CdS QDs upon the addition of a fixed concentration ( $20 \mu\text{g mL}^{-1}$ ) of commercial lipase samples.

**Table 1.** Detection of lipase activities by pH-stat potentiometric titration method and the proposed method

Lipase	Novozymes 435	PPL	CRL	FNL	PSL
$V_{\text{NaOH}} / \text{mL}$	0.883	0.695	0.626	0.513	0.426
$V_{\text{blank}} / \text{mL}$	0.051	0.017	0.028	0.032	0.045
Activity / ( $\text{U g}^{-1}$ )	4.521	3.558	3.205	2.627	2.181
RSD (n = 3) / %	2.8	4.3	3.7	3.3	5.1

Novozymes 435: Novozymes 435 lipase; PPL: porcine pancreatic lipase; CRL: *Candida rugosa* lipase; FNL: *Fervidobacterium nodosum* lipase; PSL: pseudomonas lipase;  $V_{\text{NaOH}}$ : volume of NaOH consumed during titration of the samples;  $V_{\text{blank}}$ : volume of NaOH consumed during blank titration; RSD: relative standard deviation.

## Conclusions

In summary, a colorimetric and fluorescence dual-signal sensor, depending on the IFE between MT-AuNPs and CdS QDs, for the lipase activity has been proved

here for the first time. It can achieve dual signals from one single system by utilizing different transduction principles. The high sensitivity to lipase was achieved with the LOD of  $0.039 \mu\text{g mL}^{-1}$  for colorimetric detection as well as  $0.012 \mu\text{g mL}^{-1}$  for fluorescence method. As demonstrated, this enzymatic reaction supported IFE-based sensor would break a new ground for facile and high throughput detection of enzyme activity using nanomaterials. The complicated modification of the fluorophore or covalent bond linking between receptor and fluorophore will be avoided. Furthermore, a “off-on” nano assembly for lipase determination has been proposed here which had been found few works in literature about this topic. Since the turn-on mechanism could reduce false positive results greatly and the strong fluorescence of CdS QDs can provide higher signal/background ratio, the “off-on” system will be a better choice comparing the popular turn-off sensing strategies based on the IFE. In the future, the potential of the nanomaterials such as carbon quantum dots, gold nanorod, etc., would be applied to constructing other detection platforms.

## Supplementary Information

Supplementary information is available free of charge at <http://jbcs.sbq.org.br> as PDF file.

## Acknowledgments

This work was supported by Outstanding Youth Project of National Natural Science Foundation of China (31922070).

## Author Contributions

All authors contributed equally to the article.

## References

- Kumar, A.; Khan, A.; Malhotra, S.; Mosurkal, R.; Dhawan, A.; Pandey, M. K.; Singh, B. K.; Kumar, R.; Prasad, A. K.; Sharma, S. K.; Samuelson, L. A.; Cholli, A. L.; Len, C.; Richards, N. G. J.; Kumar, J.; Haag, R.; Watterson, A. C.; Parmar, V. S.; *Chem. Soc. Rev.* **2016**, *45*, 6855.
- Jaeger, K. E.; Eggert, T.; *Curr. Opin. Biotechnol.* **2002**, *13*, 390.
- Houde, A.; Kademi, A.; Leblanc, D.; *Appl. Biochem. Biotechnol.* **2004**, *118*, 155.
- Hasan, F.; Shah, A. A.; Hameed, A.; *Enzyme Microb. Technol.* **2006**, *39*, 235.
- Chandra, P.; Enespa; Singh, R.; Arora, P. K.; *Microb. Cell Fact.* **2020**, *19*, 169.

6. Ismail, A. R.; Kashtoh, H.; Baek, K. H.; *Int. J. Biol. Macromol.* **2021**, *187*, 127.
7. Melani, N. B.; Tambourgi, E. B.; Silveira, E.; *Sep. Purif. Rev.* **2019**, *49*, 143.
8. Phukon, L. C.; Chourasia, R.; Kumari, M.; Godan, T. K.; Sahoo, D.; Parameswaran, B.; Rai, A. K.; *Bioresour. Technol.* **2020**, *309*, 123352.
9. Nomura, D. K.; Casida, J. E.; *Chem.-Biol. Interact.* **2016**, *259*, 211.
10. Shi, J.; Deng, Q.; Wan, C.; Zheng, M.; Huang, F.; Tang, B.; *Chem. Sci.* **2017**, *8*, 6188.
11. Shi, J.; Zhang, S.; Zheng, M.; Deng, Q.; Zheng, C.; Li, J.; Huang, F.; *Sens. Actuators, B* **2017**, *238*, 765.
12. Qiao, Z.; Zhang, H.; Zhang, Y.; Wang, K.; *iScience* **2020**, *23*, 101294.
13. Zhao, D. H.; Yang, J.; Xia, R. X.; Yao, M. H.; Jin, R. M.; Zhao, Y. D.; Liu, B.; *Chem. Commun.* **2018**, *54*, 527.
14. Franke, D.; Harris, D. K.; Chen, O.; Bruns, O. T.; Carr, J. A.; Wilson, M. W. B.; Bawendi, M. G.; *Nat. Commun.* **2016**, *7*, 12749.
15. Zhang, L. J.; Xia, L.; Xie, H. Y.; Zhang, Z. L.; Pang, D. W.; *Anal. Chem.* **2018**, *91*, 532.
16. Chen, J.; Sun, N.; Chen, H.; Zhang, Y.; Wang, X.; Zhou, N.; *Food Chem.* **2022**, *367*, 130754.
17. Iannazzo, D.; Espro, C.; Celesti, C.; Ferlazzo, A.; Neri, G.; *Cancers* **2021**, *13*, 3194.
18. Ji, Y.; Li, Y. M.; Seo, J. G.; Jang, T. S.; Knowles, J. C.; Song, S. H.; Lee, J. H.; *Nanomaterials* **2021**, *11*, 1446.
19. Breger, J. C.; Susumu, K.; Lasarte-Aragonés, G.; Díaz, S. A.; Brask, J.; Medintz, I. L.; *ACS Sensors* **2020**, *5*, 1295.
20. Zhang, R.; Li, N.; Sun, J.; Gao, F.; *J. Agric. Food Chem.* **2015**, *63*, 8947.
21. Zhao, Q.; Wu, D.; Yin, Z.-Z.; Cai, W.; Zhou, H.; Kong, Y.; *Anal. Methods* **2021**, *13*, 2290.
22. Yuan, P.; Walt, D. R.; *Anal. Chem.* **1987**, *59*, 2391.
23. Ray, P. C.; Fortner, A.; Darbha, G. K.; *J. Phys. Chem. B* **2006**, *110*, 20745.
24. Zhang, J.; Zhou, R.; Tang, D.; Hou, X.; Wu, P.; *TrAC, Trends Anal. Chem.* **2019**, *110*, 183.
25. Zhou, J.; Zhang, F.; Zhao, R.; Liu, S.; Li, W.; He, F.; Gai, S.; Yang, P.; *Sens. Actuators, B* **2021**, *340*, 129930.
26. Tang, Y.; Zhang, W.; Liu, J.; Zhang, L.; Huang, W.; Huo, F.; Tian, D.; *Nanoscale* **2015**, *7*, 6039.
27. Zhang, H.; Wu, S.; Zhang, L.; Jiang, L.; Huo, F.; Tian, D.; *Anal. Methods* **2019**, *11*, 2286.
28. Zhang, W.; Tang, Y.; Liu, J.; Jiang, L.; Huang, W.; Huo, F.; Tian, D.; *J. Agric. Food Chem.* **2014**, *63*, 39.
29. Zhang, W.; Liu, J.; Zhang, L.; Gan, J. h.; Ding, Y.; Huang, W.; Huo, F.; Tian, D.; *RSC Adv.* **2015**, *5*, 73051.
30. Xue, M.; Wang, X.; Wang, H.; Chen, D.; Tang, B.; *Chem. Commun.* **2011**, *47*, 4986.
31. Khezri, S.; Bahram, M.; Samadi, N.; *Anal. Methods* **2017**, *9*, 6513.
32. Chen, Y.; Rosenzweig, Z.; *Anal. Chem.* **2002**, *74*, 5132.
33. Yu, W.; Qu, L.; Guo, W.; Peng, X.; *Chem. Mater.* **2003**, *15*, 2854.
34. Pyne, S.; Sahoo, G. P.; Bhui, D. K.; Bar, H.; Sarkar, P.; Maity, A.; Misra, A.; *Sens. Actuators, B* **2011**, *160*, 1141.
35. Haiss, W.; Thanh, N. T. K.; Aveyard, J.; Ferning, D. G.; *Anal. Chem.* **2007**, *79*, 421.
36. Cui, Y.; Zhang, L.; Shi, B.; Chen, S.; Zhao, S.; *Sens. Actuators, B* **2021**, *344*, 130080.
37. George, J. K.; Ramu, S.; Halali, V. V.; Balakrishna, R. G.; *ACS Appl. Mater. Interfaces* **2021**, *13*, 57264.
38. Qi, S.; Zheng, H.; Qin, H.; Zhai, H.; *Analyst* **2020**, *145*, 3871.
39. Zhang, J.; Lu, X.; Lei, Y.; Hou, X.; Wu, P.; *Nanoscale* **2017**, *9*, 15606.
40. Yang, H.; Hao, C.; Liu, H.; Zhong, K.; Sun, R.; *J. Mol. Liq.* **2021**, *332*, 115851.
41. Cao, X.; Shen, F.; Zhang, M.; Guo, J.; Luo, Y.; Li, X.; Liu, H.; Sun, C.; Liu, J.; *Food Control* **2013**, *34*, 221.
42. Sapsford, K. E.; Berti, L.; Medintz, I. L.; *Angew. Chem., Int. Ed.* **2006**, *45*, 4562.
43. Su, K. H.; Wei, Q. H.; Zhang, X.; *Nano Lett.* **2003**, *3*, 1087.
44. Yang, X.; Yang, M.; Pang, B.; Vara, M.; Xia, Y.; *Chem. Rev.* **2015**, *115*, 10410.

Submitted: October 28, 2021

Published online: March 24, 2022

